Electric Propulsion Subsystem Optimization for "Ion Beam Shepherd" missions

IEPC-2015-IEPC-35/ISTS-2015-b-IEPC-35

Presented at Joint Conference of 30th International Symposium on Space Technology and Science, 34th International Electric Propulsion Conference and 6th Nano-satellite Symposium
Hyogo-Kobe, Japan
July 4–10, 2015

F. Cichocki*, M. Merino†
and E. Ahedo‡
Equipo de Propulsión Espacial y Plasmas (EP2), Universidad Carlos III de Madrid, Spain
D. Feili§
University of Southampton, Southampton, SO17 1BJ, United Kingdom
and
M. Ruiz¶
SENER Ingeniería y Sistemas, Tres Cantos, Madrid, Spain

The Ion Beam Shepherd (IBS) is an innovative contactless technique for space debris removal, in which an Impulse Transfer Thruster (ITT) exerts a force on the debris object by directing a plasma plume towards it. The optimal operational points of the ITT and of the impulse compensation thruster (ICT) needed for formation flying, strongly depend on the physics of the ITT plume expansion into vacuum, so that a dedicated study is needed. A simplified model for the ITT plume expansion and interaction with the debris is described and used to estimate the momentum transfer efficiency, or the fraction of thrust transferred to the debris object. With the use of dedicated ITT and ICT thruster performance models, a system level optimization study of the overall electric propulsion subsystem is then presented for a specific IBS mission, discussing how the plume expansion physics affects the results.

Nomenclature

α_0	= Initial divergence angle of the 95% ion current streamtube
α_F	= Far region divergence angle of the 95% ion current streamtube
α_{pwr}	= Specific mass of the solar array
η_B	= Momentum transfer efficiency
η_{PPU}	= Energy conversion efficiency of the Power Processing Unit
γ	= Electron polytropic cooling coefficient
η_B	= Momentum transfer efficiency
Δt_{IBS}	= Duration of the IBS shepherding phase
ΔV_{tot}	= Total delta-V of the shepherding phase (excluding attitude control)
d	= Distance between the thruster and the geometrical centre of the target debris
d_0	= Axial extension of the near region of the plasma plume

*PhD student, Bio-engineering and Aerospace Engineering Department, filippo.cichocki@uc3m.es
†Associate professor, Bio-engineering and Aerospace Engineering Department, mario.merino@uc3m.es
‡Professor, Bio-engineering and Aerospace Engineering Department, eduardo.ahedo@uc3m.es
§Senior Lecturer, Astronautic Research Group, D.Feili@soton.ac.uk
¶Project Manager, Aerospace Department, mercedes.ruiz@sener.es

e = Electron charge
f = Fraction of the orbit in daylight conditions
F_{debris} = Transmitted force to the debris
F_{ICT} = Thrust of the impulse compensation thruster
F_{ITT} = Thrust of the impulse transfer thruster
g_0 = Standard gravity acceleration
h = Self-similarity function modelling the radius of the ion streamline
$I_{sp\ eq}$ = Equivalent specific impulse of the electric propulsion subsystem
I_{spITT},I_{spICT} = Specific impulse of the ITT and ICT
n,n_0 = Plasma plume number density and its value at the origin
M_0 = Plasma plume ion Mach number
m_{ISC} = Mass of the ion beam shepherd spacecraft
m_{TG} = Mass of the space debris
m_{power} = Total mass of the power generation subsystem
m_{prop} = Total propellant mass for the shepherding phase
$\dot{m}_{ITT}$,$\dot{m}_{ICT}$ = Mass flow rates of the impulse transfer and impulse compensation thrusters
q_i = Electric charge of the ions, assumed to be equal to the electron charge e
(r, z) = Radial and axial coordinate in the plasma plume reference frame
$\tilde{r}$,$\tilde{z}$ = Normalized radial and axial coordinate in the plasma plume reference frame
P_{tot} = Total input power to the thrusters
R_0,R_F = Initial and final radius of the 95% ion current streamtube
R_{thr} = Thruster radius, here assumed equal to R_0
R_{TG} = Radius of the equivalent spherical target debris
T_e,T_{e0} = Electron temperature and its value at the origin
u_z, u_0 = Plasma plume axial velocity and its value at the origin
u_r = Plasma plume radial velocity
V_{beam} = Effective acceleration voltage of the ITT plasma beam

I. Introduction

THE space debris problem has been drawing an increasing level of attention in the scientific community in the last decade. The exponentially increasing number of space debris objects that populate certain types of orbits (especialy the Sun Synchronous Low Earth Orbits and the Geostationary orbits) could potentially threaten their exploitation in a relatively close future,[1,2] and therefore, demands an international effort in two major fields: mitigation strategies and active debris removal/relocation.

First of all, it is paramount to define common and international disposal strategies at the end of life of both commercial and scientific satellites. This represents an extra cost to be added to the mission budget (e.g. extra propellant to transfer the satellite from its operative orbit to a disposal orbit) and therefore it is crucial that it be common to all space competitors in the international scene.

Secondly, efforts have to be put into investigating and demonstrating the technical feasibility of active debris removal (ADR) techniques, which could potentially lower the cost of the necessary disposal strategies and/or reduce the debris concentration levels in particularty saturated orbits. Among many proposed techniques for ADR, the Ion Beam Shepherd[3–5] is being considered as a serious candidate by the European Commission, which is currently financing a project named LEOSWEEP ("Improving Low Earth Orbit Security With Enhanced Electric Propulsion"[6]), its major goals being the study of the technical feasibility of the IBS technique and the advance in the design of the related technologies.

The Ion Beam shepherd concept is briefly described hereafter. Referring to Fig.1, an Ion Beam Shepherd S/C (ISC) makes use of an onboard electric thruster to direct a plasma beam against a target debris. The impact of the hypersonic ions of the plume produces a net force on the target, which can be repositioned "contactlessly" into a different disposal orbit.

However, because of the radial plume expansion,[7,8] the operating distances are limited to approximately

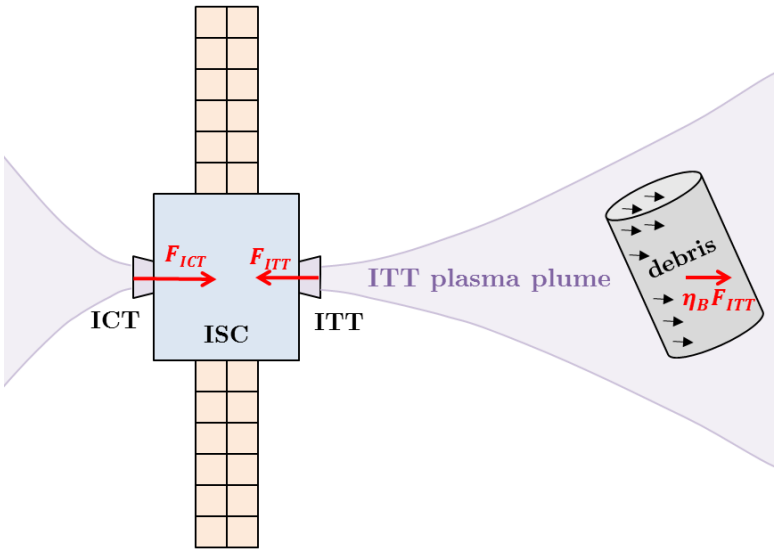

Figure 1. Schematic of the Ion Beam Shepherd Concept.

7-15 metres and strongly depend on the target size and on the divergence angle of the electric thruster. The effective force transferred to the debris is thus only a fraction of the total ITT thrust F_{ITT}, as shown in Eq.1, with η_B representing the momentum transfer efficiency:

$$F_{debris} = \eta_B \cdot F_{ITT}, \tag{1}$$

In order to maintain formation flying, the Impulse Transfer Thruster (ITT) has to be compensated by an Impulse Compensation Thruster (ICT), which is located on the opposite side of the S/C. More precisely, formation flying demands that the accelerations on both the ISC and the space debris be equal, meaning that the ICT thrust F_{ICT} is generally higher than that of the ITT,[9] as dictated by Eq.2, where m_{ISC} and m_{TG} are respectively the ISC and target debris masses.

$$F_{ICT} = \left(1 + \eta_B \cdot \frac{m_{ISC}}{m_{TG}}\right) \cdot F_{ITT} > F_{ITT}, \tag{2}$$

In the frame of the LEOSWEEP project, an optimal Radio Frequency Ion Thruster (RIT) is being developed for the ITT.[10] The ICT type, on the other hand, is currently being traded off, with feasible options being another RIT or an existing Hall Effect thruster. The operating conditions of the two thrusters (e.g. the operating voltage and the thrust), strongly depend on the distance between the ISC and the debris object and on the mission delta-V.

For the ITT, at a fixed thrust, both the momentum transfer efficiency and the required power grow with the thruster specific impulse. The former grows because, the higher the specific impulse, the lower the plume divergence angle and hence the fraction of ions impacting the debris, while the latter grows because the ions are accelerated to higher speeds. Therefore, an optimal specific impulse must exist that maximizes the transferred thrust to power ratio, a very important figure of merit in an IBS mission. For the ICT, on the other hand, the sum of the required propellant mass and dedicated power system mass should be minimized, without any particular concern on the thruster divergence angle.

At system level, it is therefore paramount to identify the optimal operational points of both thrusters that can yield the lowest possible system mass, while complying with a vast set of constraints, ranging from overall power availability to size and cost of the required components. The paper's main goal is thus to propose an approach for the IBS electric propulsion subsystem optimization, considering a real space mission scenario, like that of the LEOWSEEP demonstration mission.

Before proceeding with the description of this overall subsystem optimization, the mission facts and requirements are introduced in Sec.II, while the ITT and ICT performance models considered in the analysis are introduced in Sec.III. Then, the simplified models for the plasma plume expansion and interaction with

the space debris are described in Sec.IV. The optimization of the ITT alone is briefly described in Sec.V, with a discussion of the influence of the plume expansion physics on the optimal operation point. Sec.VI then presents the results of the overall propulsion subsystem optimization, taking into account the total thrusters power, the propellant and the dedicated power subsystem mass. Finally, the conclusions of the study are reported in Sec.VII.

II. Mission Constraints and Propulsion Subsystem Requirements

The current specifications of the LEOSWEEP mission are summarized in Tab.1. The preliminary debris object is a launcher upper stage of approximately 1.5 tons mass, orbiting in a nearly polar Low Earth Orbit (LEO). In order to prove the feasibility of the IBS technique, a de-orbiting manoeuvre of approximately 300 km in 170 days has been considered as the baseline mission goal. This means that the ISC must de-orbit the debris at a rate of approx. 2 km/day. Considering an average 67% orbit daylight fraction (thrusters cannot operate on battery power alone, due to a S/C design choice), this is equivalent to imposing a constraint on the transmitted force on the debris: 30 mN.

Table 1. De-orbiting mission specifications

Mission facts	Units	Values
Debris mass	tons	~ 1.5
Orbit altitude change	km	~ 300
Required altitude change per day	km/day	~ 2
Daylight fraction in orbit	%	67
Shepherding phase duration	days	170

This force requirement and other additional requirements and constraints on the electric propulsion subsystem (EPS), are finally listed in Tab.2. The minimum distance between the ITT exit plane and the debris object has been set to 7 m (the half span of the S/C solar array) in order to avoid collisions between the ISC and the target debris in case of a failure of the relative attitude control. Moreover, the electric power platform design limits the total input power to the Power Processing Unit (PPU) of the EPS to 3 kW, which is equivalent to approx. 2.6 kW of total thruster power (ITT plus ICT), after assuming a PPU efficiency of 85%.

Table 2. EPS requirements and constraints

EPS requirements and constraints	Units	Values
Required force on the debris, F_{debris}	mN	30
Operational distance between ITT and debris	m	> 7
Input power to the EPS PPU	kW	~ 3
PPU efficiency	%	85
Input power to both thrusters	kW	~ 2.6

III. Characterization of ITT and ICT

As already mentioned in Sec.I, the ITT for the LEOSWEEP mission is a Radio-frequency Ion Thruster (RIT) and its test prototype is being designed and manufactured within the LEOSWEEP project.

The RIT is a particular type of Gridded Ion Thruster (GIT). In GITs, the thrust is generated through the action of static electric fields, which accelerate the plasma ions (refer to Fig.2) through a ion optics system. The positive charge of the emitted ions is to be compensated with an external electron source, or a neutralizer. In the acceleration process, ions acquire a kinetic energy given by $q_i V_{beam}$, with q_i representing the ion charge and V_{beam} the effective acceleration beam voltage (which we shall refer to as beam voltage in the rest of the paper). Such beam voltage is almost equal to the positive screen grid voltage with respect to

the S/C ground, with a difference of just a few 10s of volts.

What really distinguishes a RIT from a GIT, however, is the propellant gas ionization, that is achieved through the action of a megacycle electromagnetic field. For this purpose, two components are needed: an ionization chamber made of insulating material and an RF coil surrounding such chamber. When an RF current flows in the coil, an alternating axial magnetic field is generated and, in turn, through Faraday's law, an azimuthal, circular electric field is induced. Such field accelerates the free electrons to energies high enough to ionize the neutral gas atoms. The input power of a RIT can thus be split into two contributions: RF and beam power. The former is the power of the generator required to produce the megacycle current of the RF coil and hence the plasma. The latter is the high voltage supply power needed to transport electrons from the very high potential of the screen grid to the neutralizer and then to the plasma plume. In fact, in stationary conditions, the electron current absorbed by the screen grid must be equal to the ionic beam current flowing through the ion optics system.

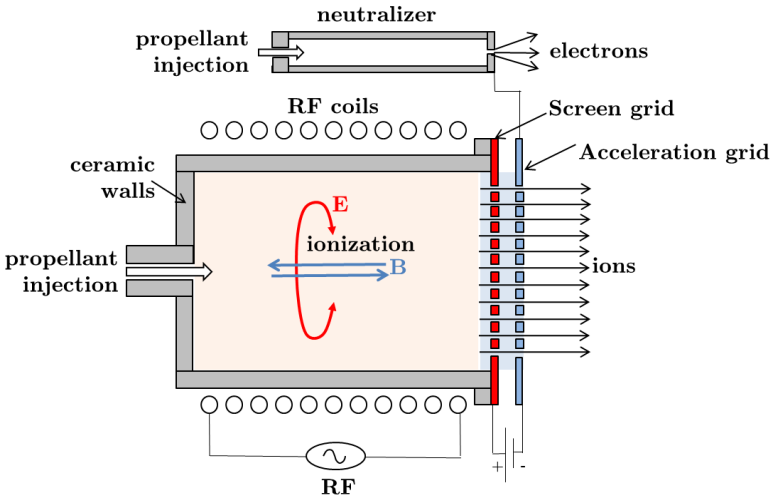

Figure 2. Generic working principle of a RIT thruster

In order to begin this optimization study, a thruster performance model is needed to explore the behavior of thruster figures of merit such as the beam divergence angle, the mass flow rate or the required total thruster power as a function of some design parameters. This performance model should not be interpreted as a specific thruster performance model.

Details on the ITT performance model used herein can be partially found in Ref.10. Summarizing the results of that study, such a performance model allows computing the different figures of merit of the ITT as a function of the beam voltage V_{beam} and of the ITT thrust T_{ITT} (which sizes the thruster). The most important functional dependencies are summarized below:

- The divergence angle decreases sensibly with the beam voltage as $\alpha_0 \propto V_{beam}^{-\beta}$ with $\beta > 1$
- The total power grows almost linearly with T_{ITT} at constant V_{beam}, and with V_{beam} at constant T_{ITT}
- The thrust efficiency increases slightly with both T_{ITT} and V_{beam} with an average value around 50%
- The specific impulse is almost a function of the sole V_{beam}, with a very small increase with T_{ITT} at a fixed V_{beam}. Ideally, the specific impulse should go as $I_{spITT} \propto V_{beam}^{1/2}$ for a constant propellant utilization efficiency

For what concerns the ICT characterization, for this optimization study, a RIT type thruster has been considered as well. This is something that has not been frozen yet in the design process. Nevertheless, it is a reasonable choice as installing the same type of thruster for both ITT and ICT clearly reduces the system complexity. The ICT design performance model is finally similar to that of the ITT, with more details to be found also in Ref.10.

IV. Modeling the momentum transfer efficiency

A. Simplified plume expansion and debris interaction models

A detailed description of the physical phenomena taking place in a plasma plume expansion into vacuum is provided in Refs.7 and 8. In summary, the plasma plume generated by a plasma thruster can be divided into two regions as sketched in Fig.3. First, a near region extending up to a few thruster radii from the thruster exit where collisions, thruster electromagnetic fields and neutralizer 3D effects dominate the expansion, and where beamlets coalescence into a single-peaked beam take place. Second, a far region plume, where these effects become negligible and the smooth, single peaked profile continues to expand under the influence of the residual electron pressure and of the ambipolar electric field. The complex near-region plume cannot be easily modelled in terms of simple equations, and it is usually characterized experimentally. The far-region plume, on the other hand, can be studied with simplified fluid models. These models are presented and discussed in detail in Refs.7 and 8 and are employed here to study the effect of the plume expansion.

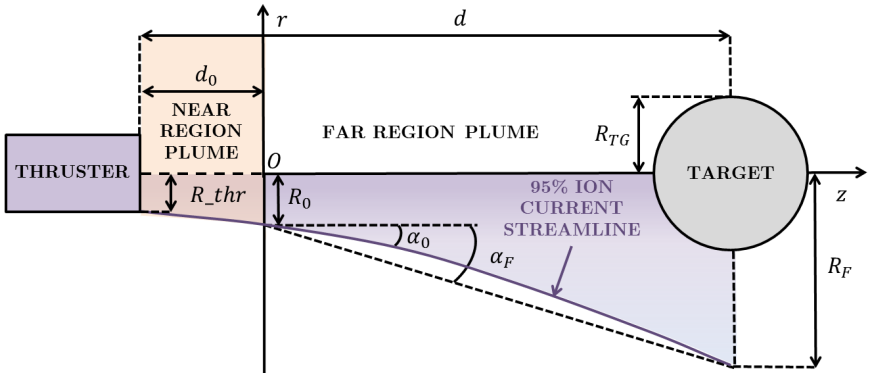

Figure 3. Sketch of a plasma plume near and far regions, and the plasma streamtube containing 95% of the ion current

Referring to Fig.3, we begin by defining a reference frame based on an initial plane located within the far region at a distance d_0 from the thruster exit, sufficiently large to cover the near-region. Existing experimental observations of gridded ion thrusters and Hall effect thrusters show that the plume has already become smooth and single-peaked after less than one or two thruster radii from the thruster exit.[11–13] Following the self-similar plume solution method, firstly introduced by Park[14] and generalized in Refs.7 and 8, at this initial plane, the plume is assumed to have a Gaussian density profile and a velocity profile featuring a constant axial velocity component $u_z(r, z = 0) = u_{i0}$ and a linearly increasing radial velocity $u_r(r, z = 0) = u_{i0} \cdot (r/R_0) \cdot \tan\alpha_0$. Here, R_0 and α_0 represent the radius and the half-angle of the streamtube containing 95% of the ion current at the initial plane, as shown in Fig.3. The method then allows to compute the 95% ion current streamline radius $R(z)$, the axial and radial plume velocity $u_z(r, z)$ and $u_r(r, z)$, and the plume density $n(r, z)$, as shown in Eqs.3 to 6, with n_0 and u_{i0} the plasma density and ion velocity at the origin O and h a self-similarity function, whose derivative h' is with respect to $\tilde{z} = z/R_0$:

$$R(z) = R_0 \cdot h(z/R_0) \tag{3}$$

$$u_z(r, z) = u_{i0} \tag{4}$$

$$u_r(r, z) = u_{i0} \cdot h'(z/R_0) \cdot \frac{r}{R(z)} \tag{5}$$

$$n(r, z) = \frac{n_0}{h^2(z/R_0)} \exp\left(-3\left[r/R(z)\right]^2\right) \tag{6}$$

The unknown self-similarity function $h\,(z/R_0)$ can be computed through numerical integration, after introducing two fundamental plume parameters: the effective electron polytropic cooling coefficient γ,[7,8] expressing the relation between electron temperature and density $T_e \propto n^{\gamma-1}$ and the ion Mach number, whose square represents the ratio between the ion kinetic energy and the electron thermal energy, as shown in Eq.7, where m_i and T_{e0} represent respectively the ion mass and the electron temperature at the origin O of the reference frame of Fig.3

$$M_0 = \sqrt{\frac{m_i u_{i0}^2}{\gamma T_{e0}}} = \sqrt{\frac{2eV_{beam}}{\gamma T_{e0}}} \tag{7}$$

The self-similarity function h can then be solved in terms of M_0, γ and $\alpha_0 = h'(0)$, by integrating Eq.8 along $\tilde{z}$, with the initial condition $h(0) = 1$:

$$(h')^2 - (h'(0))^2 = \frac{6}{M_0^2} \times \begin{cases} -\left(h^{2-2\gamma} - 1\right) / (\gamma - 1) & \text{for } \gamma > 1, \\ 2 \ln h & \text{for } \gamma = 1. \end{cases} \tag{8}$$

Note, finally, that the plume radius $R(z)$ depends both implicitly (through h) and explicitly on R_0 through Eq.3. The same applies for the velocity and density.

With the plume solution of Eqs.3 to 6 and following the approach of Ref.9, it is finally possible to obtain an analytical formula for the fraction of plume momentum intercepted by the debris. This is modelled as an equivalent sphere of radius R_{TG}, with d representing the operational distance between the thruster exit and the centre of the sphere. At this distance, the radius of the plasma tube carrying 95% of the ion current is R_F, which allows us to define an equivalent conical far region divergence angle α_F as:

$$\alpha_F = \arctan\left(\frac{R_F - R_0}{d - d_0}\right) \tag{9}$$

Note that α_F is not the local angle of the 95% ion current streamline, as clearly shown in Fig.3. Integrating the plasma momentum over the surface of the sphere,[9] we can finally compute the momentum transfer efficiency as:

$$\eta_B = 1 - \exp\left(-\frac{3 \cdot R_{TG}^2}{\left(R_0 + (\tan\alpha_F) \cdot (d - d_0)\right)^2 - \left(\tan\alpha_F \cdot R_{TG}\right)^2}\right) \tag{10}$$

Note that Eq.10 could also be expressed in terms of R_F through Eq.9. Being R_0, d and d_0 fixed parameters, there is indeed a biunique relation between α_F and R_F.

Given the impossibility to obtain experimental near region data at this design stage of the project, we shall here consider that our far region starts at the exit plane of the thruster ($d_0 = 0$), where numerical simulations have been carried out to characterize the divergence angle α_0.[10] To cover for the potential divergence increase caused by the near-region, we shall therefore include a +10% margin on this initial divergence angle (or thruster divergence angle) with respect to the data at the thruster exit plane.

All the parameters affecting the calculation of the momentum transfer efficiency are finally summarized in Tab.3.

Table 3. Parameters affecting the plume expansion and target interaction

Plume and debris interaction parameters	Units	Values
Polytropic electron cooling coefficient γ	n/a	1.0
Electron temperature T_{e0} at the origin O	eV	3.0
Equivalent spherical radius R_{TG} of the debris	m	1.25
Near region axial length d_0	m	0.0
Distance between thruster exit and debris centre	m	7.0
Xenon propellant ion mass m_i	kg	$2.18 \cdot 10^{-25}$
Xenon ion charge e	C	$1.6 \cdot 10^{-19}$

Here, the polytropic electron cooling coefficient and the initial electron temperature allow us to compute the ion Mach number and, hence the final radius R_F of the 95% ion current streamtube with the plume model described above. In electric propulsion devices, typical far-region electron temperatures are around 2-3 eV[11,12] for Hall Effect thrusters and between 1 and 3 eV for Ion thrusters.[13] The same authors suggest the use of a polytropic cooling coefficient between 1.1 and 1.3 to model the electron temperature decrease as the plume expands. In our study, we have therefore assumed conservative values, that is an electron temperature

of 3 eV, with zero cooling rate ($\gamma = 1.0$). This corresponds to the worst case scenario in terms of momentum transfer efficiency. In fact, the closer to isothermal are the electrons (contolled by γ) and the higher their thermal energy (controlled by T_{e0}), the farther downstream they retain their thermal pressure thus making the ion streamlines diverge more.[7,8] Therefore, the lower the γ and the higher the T_{e0}, the higher the α_F and, consequently, the lower the η_B (through Eq.10). The reported spherical envelope radius R_{TG} is the equivalent spherical envelope of the upper stage target of the LEOSWEEP mission and the distance d has been assumed equal to the lower limit of the operational distance of Tab.2. Finally, singly-charged Xenon ions are assumed to constitute the plasma plume.

B. Far region divergence angle and momentum transfer efficiency

Before proceeding with the optimization study, the effect of the ITT beam voltage on both the far region divergence angle and consequently on the momentum transfer efficiency has to be assessed.

With the use of the plume model described in Sec.IV A and for an operational distance $d = 7m$ and an initial plume radius $R_0 = R_{thr} = 7$ cm, we can obtain a 2-D map of the far region divergence angle as a function of V_{beam} and α_0.

Referring to Fig.5, as the beam voltage or the near region divergence angle increase, the difference between the near and far region divergence angles becomes smaller. Asymptotically, α_F tends to α_0 for both increasing beam voltage V_{beam} and near region divergence angle. Since, for our ITT performance model, the near region divergence angle α_0 is a direct function of the beam voltage, the actual far region divergence angle is also a single variable function of the ITT beam voltage.

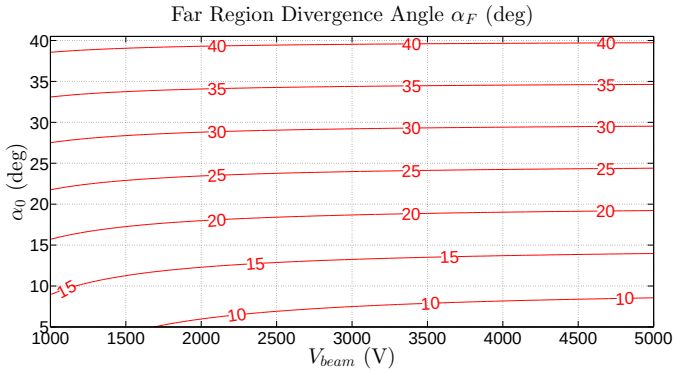

Figure 4. Dependency of the far region divergence angle on the acceleration beam voltage V_{beam} and on the ITT divergence angle α_0

The far region divergence angle also depends on the initial plasma plume radius (or equivalently on the thruster radius). Since this is a design study, such a radius is not known a priori, so α_F has been evaluated for a set of different thruster radii, whose range should include our final design solution (7, 15 and 25 cm). The worst case (highest α_F) corresponds to the lowest thruster radius (7 cm), due to larger radial density gradients. In other words, the lower the initial thruster radius, the higher is the normalized distance of the debris from the thruster (z_F/R_0) and hence the higher is the divergence increase of the plume. Being conservative, this 7 cm case has been considered to compute a numerical fitting of α_F versus V_{beam}.

Such a conservative numerical fitting can be found in Ref.10 and has been used in Eq.10 to compute the ITT momentum transfer efficiency as a function of the beam voltage for the same set of thruster radii, as shown in Fig.5.

In this case, a higher thruster radius appears to lower the momentum transfer efficiency. This might seem to be counterintuitive, as the far region divergence angle was lower for those cases. However, since we have considered the worst case fitting for the far region divergence angle, the only acting parameter as the thruster radius changes, is the R_0 term appearing explicitely in Eq.10. The higher this radius, the higher the plume radius at the target and hence the lower the overall momentum transfer efficiency.

In the remaining part of the optimization study, we shall therefore be conservative once again and assume the worst case thruster radius of 25 cm, when computing the ITT momentum transfer efficiency.

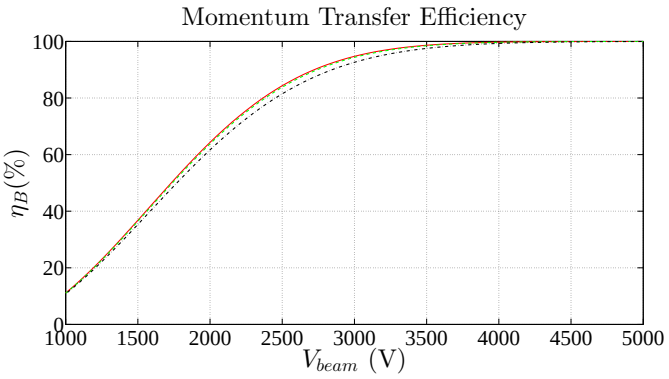

Figure 5. Momentum transfer efficiency η_B as a function of the ITT beam voltage V_{beam} for various thruster radii: 7 cm (red solid line), 15 cm (green dashed line), 25 cm (black dash-dot line)

V. Optimization of the ITT

A. The main figures of merit of the ITT

The optimization of the ITT design point in terms of the beam voltage is briefly summarized in this subsection. By fixing the transmitted force on the target to the required 30 mN value (see Tab.1), it is straightforward to compute the required ITT thrust as a function of its beam voltage as $F_{ITT}(V_{beam}) = 30\ \text{mN}/\eta_B(V_{beam})$. Hence, once V_{beam} is fixed, all the thruster performance figures can be easily obtained with the ITT performance model of Ref.10.

The study carried out in Ref.10 identifies as a key figure to maximize, the ratio between the transmitted force and the corresponding thruster power. For low beam voltages and hence momentum transfer efficiencies (refer to Fig.5), the required ITT thrust decreases almost linearly with V_{beam}, while the ITT thruster power grows approximately with its square root. This means that the transmitted force to power ratio keeps growing with V_{beam} until reaching a maximum, that represents a good candidate for the optimal operational ITT beam voltage.

Nevertheless, the choice of the design voltage of the ITT cannot be determined solely by the maximization of this performance figure. Another factor affecting the beam voltage choice is the required propellant mass, which clearly reduces with the beam voltage or, equivalently, with the specific impulse (remember that, ideally, $I_{sp} \propto V_{beam}^{1/2}$).

Finally, the propellant utilization efficiency, which is seen to decrease with the beam voltage, should be high enough not to yield an excess of neutral outflow. In fact, this would cause a high number of charge-exchange collisions with the plume ions, and hence a large ion backflow towards sensitive S/C surfaces, which could potentially endanger the mission, or increase the initial plume divergence beyond the values assumed here.

B. The role of the plasma plume expansion on the ITT design

The plasma plume expansion into vacuum clearly affects the momentum transfer efficiency and, consequently, the ITT design point. The major physical processes taking place as the plume expands are described hereafter.

First of all, the plume becomes more and more rarefied due to its conical expansion. The initial plume divergence, in fact, has the effect of reducing the plume density axially as the plume gets farther from the thruster, and this reduction goes with the square of the streamline radius. So, depending on the operational distance between the ISC and the target debris object, it is paramount to minimize the initial divergence angle, which genearally requires operating at a high beam voltage.

Secondly, even if the initial divergence angle (or the thruster divergence) is small, the residual electron pressure makes the plume expand further, meaning that the slope of the ion streamlines increases away from the thruster.[7,8] This effect can be mitigated by increasing the operating Mach number of the thruster, provided by Eq.7. For a fixed propellant atom mass, this can be achieved by either increasing the beam voltage or reducing the residual electron temperature T_{e0}. For this reason, in the context of the LEOSWEEP

project, the ITT thruster is being designed specifically to reduce this residual electron temperature, a fact that has scarcely been investigated in the past and that will need to be demonstrated experimentally. In any case, the parameter to be maximized to limit the electron pressure effects is the ion Mach number, so increasing the beam voltage remains a valid solution.

Both the above discussed effects can be observed in Fig.6 (a). The momentum transfer efficiency increases substantially for decreasing divergence angles, and, for a given thruster divergence angle α_0, it shows a weak dependence on the beam voltage V_{beam}, especially at low voltage. This effect is due to the electron pressure and, for the voltage range considered here, it is quite small. The electron pressure effects can be further explored in Fig.6 (b), showing the momentum transfer efficiency dependency on the polytropic cooling coefficienct γ and on the initial electron temperature T_{e0}. This contour plot has been obtained for a fixed beam voltage V_{beam}=2000 V and an initial divergence angle $\alpha_0 = 10$ deg. Clearly, a higher electron temperature means a lower ion Mach number and hence yields a lower momentum transfer efficiency. The opposite consideration applies to γ, the isothermal case $\gamma = 1$ yielding the most conservative results (or the lowest momentum transfer). For this reason, the ITT optimization has been carried out assuming $\gamma = 1$, as already commented in Sec.IV A and shown in Tab.3.

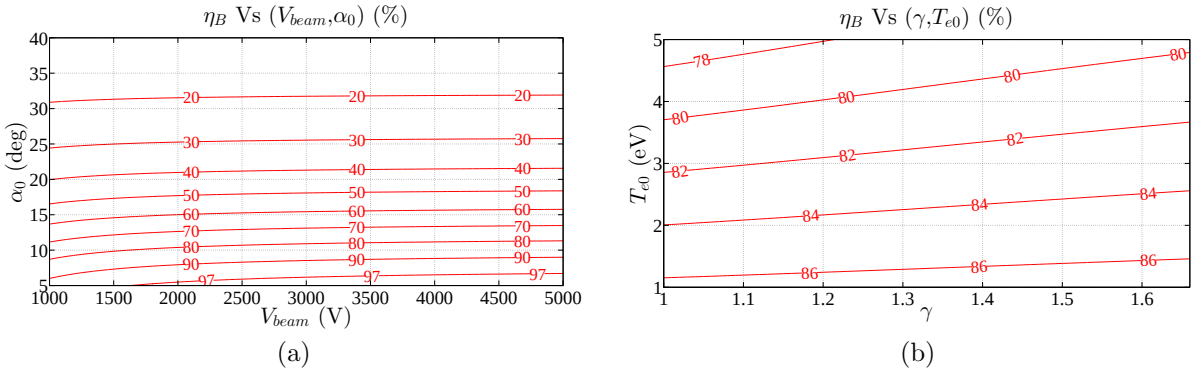

(a) (b)

Figure 6. (a) Momentum transfer efficiency η_B as a function of beam voltage V_{beam} and thruster divergence angle α_0, for $\gamma = 1.0$, $T_{e0} = 3$ eV, $R_0 = R_{thr} = 25$ cm and $d = 7$ m. (b) Momentum transfer efficiency η_B as a function of γ and T_{e0} for a fixed beam voltage $V_{beam} = 2000V$, thruster divergence angle $\alpha_0 = 10$ deg, $R_0 = R_{thr} = 25$ cm and $d = 7$ m

VI. Optimization of the electric propulsion subsystem

A. Major assumptions

What was described in Sec.V provides very valuable inputs for the choice of the operational point of the ITT alone. Nevertheless it is limited from an overall subsystem perspective, in which, what needs to be really minimized are the total dedicated mass and power of the electric propulsion subsystem. These present various contributions: the two thrusters, the overall dedicated power subsystem (solar arrays fraction dedicated to the generation of the input power to the thrusters), the overall propellant and the power processing units (PPUs).

In this section, we shall describe the approach we have followed to define the optimal operational points of both thrusters simultaneously, defined, once again, in terms of their beam voltage.

The parameters of Tab.2 have been considered for this study. In addition, we have considered a photovoltaic power subsystem featuring a specific mass of 13.3 kg/kW and a total ISC wet mass of 500 kg. These values appear to be representative enough for respectively the current solar array technologies and the expected design mass of the S/C.

Moreover, in order to simplify the analysis, the thrusters and PPU masses have not been included in the analysis, as their variations with the operational voltage of both thrusters is expected to be quite small. The former would slightly depend on the beam voltages of the ITT and ICT, as a higher voltage generally yields a lower required mass flow rate and hence a smaller and lighter thruster.[10] However, a thruster unit weighs only a few kg (for these power levels) and so its mass can be neglected with respect to the major mass contributions, which are the propellant mass and the dedicated power generation subsystem mass. Regarding the PPUs, on the other hand, their mass can hardly be modelled as a function of the thruster

beam voltage and, in any case, we expect that their mass variations can be neglected.

B. Overall Optimization Method

The electric propulsion subsystem optimization consists in studying the evolution of figures of merit such as the total thruster power, the total propellant mass, the dedicated power generation subsystem mass and the total delta-V as 2-D functions of the beam voltages of both the ITT and the ICT. For any ITT beam voltage:

1. The ITT thruster parameters are computed following the approach of Sec.V
2. Given the ITT thrust, the required ICT thrust is obtained through Eq.2
3. For a varying ICT beam voltage in a range between 500 and 5000 V, the following parameters are computed:
   - The ICT thruster performance figures
   - The overall (ITT+ICT) input power P_{tot}
   - The overall required propellant mass, using Eq.11, where f is the fraction of daylight in orbit given in Tab.1, Δt_{IBS} is the shepherding phase duration, and $\dot{m}_{ITT}$, $\dot{m}_{ICT}$ are the total mass flow rates of the ITT and ICT:

$$m_{prop} = f \cdot \Delta t_{IBS} \cdot (\dot{m}_{ITT} + \dot{m}_{ICT}) \tag{11}$$

   - The overall power subsystem mass, using Eq.12, where P_{tot} is the total thrusters input power (sum of the ITT and ICT thrust powers), η_{PPU} is the electrical efficiency of the PPUs (given in Tab.2) and α_{pwr} is the specific mass of the solar arrays (13.3 kg/kW)

$$m_{power} = \alpha_{pwr} \cdot P_{tot}/\eta_{PPU} \tag{12}$$

   - The total shepherding phase ΔV_{tot}. An equivalent propulsion subsystem specific impulse is firstly obtained as:

$$I_{sp,eq} = \frac{(\dot{m}_{ITT} \cdot I_{spITT} + \dot{m}_{ICT} \cdot I_{spICT})}{(\dot{m}_{ITT} + \dot{m}_{ICT})} \tag{13}$$

     where I_{spITT} and I_{spICT} are respectively the ITT and ICT specific impulses. Then, through Tsiolkovsky's equation, the total ΔV_{tot} is computed as:

$$\Delta V_{tot} = I_{sp,eq} \cdot g_0 \cdot \ln\left(\frac{m_{ISC}}{m_{ISC} - m_{prop}}\right) \tag{14}$$

     where g_0 is the standard gravity acceleration.

C. Overall Optimization Results

Following the procedure described in the previous paragraph, several figures of merit of the required EPS have been obtained as 2-D maps in the plane defined by the ITT-ICT beam voltages. These are shown in Fig.7.

Fig.7 (a) shows the overall power (after the PPUs). For a given ITT voltage, the overall power presents a minimum at an ICT voltage of approx. 1000 V. Then it starts to increase because, for a given ICT thrust (or voltage), the required ICT power grows with the ICT specific impulse (and hence with the ICT beam voltage). The point of lowest overall power in terms of ITT voltage is around 4 kV. The corresponding minimum power is 2.58 kW, achieved at the ITT-ICT voltage point (3925, 1000) V. It is important to underline that small changes in the ITT voltage around this optimal point produce no significant variation in the overall thruster power. For example a lower and "safer" ITT voltage of 3500 V would yield an overall power only 20 W higher than the above defined minimum.

Fig.7 (b) shows the overall mass dedicated to the propellant and the power generation subsystem. The optimal point shifts to higher voltages for both the ITT and the ICT with respect to that of Fig.7 (a), because the overall propellant mass reduces for increasing voltages. The optimal voltages (corresponding to

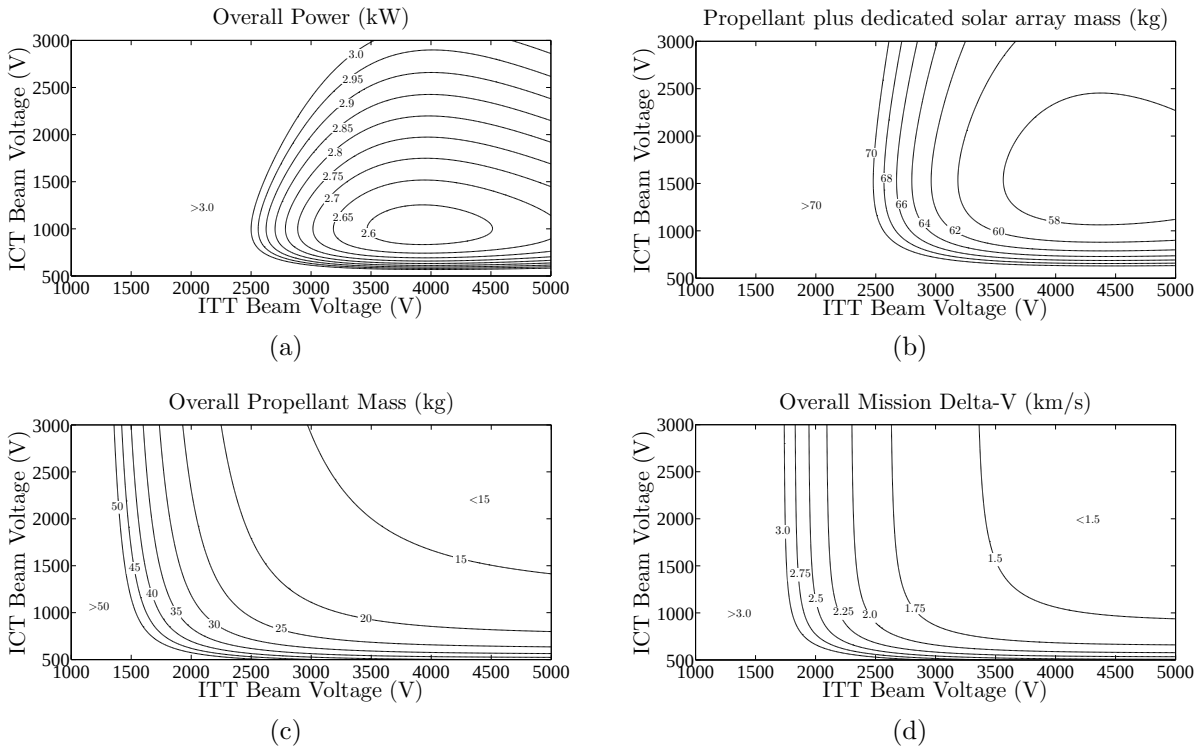

Figure 7. (a) Overall dedicated power to the propulsion subsystem. (b) Sum of the propellant and dedicated power subsystem masses. (c) Overall propellant mass of the shepherding phase.(d) Overall shepherding delta-V cost.

a total mass of 56.8 kg) are (4360, 1540) V. Observe that, for a very wide region around this optimal point, variations in both the ITT and ICT voltage produce no significant changes in the total mass.

Fig.7 (c) shows the overall propellant mass as a function of both the ITT and the ICT beam voltages. Clearly, the higher these voltages, the lower the overall propellant mass. The iso-propellant lines thus resemble the shape of a rectangular hyperbola. However, although, for a given ITT voltage, increasing the ICT voltage can reduce the overall propellant mass, such saving is quite small. For example, for an ITT voltage of 3500 V, increasing the ICT voltage from 1000 to 2000 V yields a mass saving of only 5 kg.

Finally Fig.7 (d) shows the total propulsive ΔV of the IBS shepherding phase. As expected, for an ICT voltage above 1000-1500 V, the mission delta-V depends essentially on the momentum transfer efficiency and hence on the ITT voltage alone: the higher the ITT voltage, the lower the total mission ΔV. At low ICT voltages however, the divergence loss of the ICT becomes important and this means that the ICT mass flow necessary to achieve the required thrust increases as the voltage decreases. For this reason, the total ΔV raises substantially as the ICT voltage becomes smaller.

The main conclusion that can be extracted from the presented results is that the optimal points for ICT and ITT voltage are very different. The need to guarantee a sufficiently high momentum transfer efficiency drives the optimal ITT voltage to very high values. For the ICT, on the other hand, as long as the thruster efficiency is not strongly affected, the lower the voltage the lower the required power, but the higher the propellant mass consumption. This results into an optimal beam voltage, which is generally quite lower than that of the ITT.

The optimal design choice may be either based on the total dedicated mass or on the total thruster power, depending on the specific mission constraints. For example, for missions featuring a well defined limit for the total platform power, minimization of the total thruster power should be pursued (Fig.7 (a)). For other missions not featuring such a stringent constraint, the total dedicated mass would represent a more adequate figure of merit for the overall electric propulsion subsystem (Fig.7 (b)).

VII. Conclusions

This paper has presented a study dedicated to the optimization of the electric propulsion subsystem for an Ion Beam Shepherd Mission (IBS). The IBS is a novel technique for contactless debris de-orbiting/relocation and requires two electric thrusters: an impulse transfer thruster (ITT) and an impulse compensation thruster (ICT). The optimal operational points of both thrusters, in terms of their voltage, have been identified and the corresponding optimization method described.

The dedicated design performance models of Ref.10 have been specifically used to explore the effects of changing the operational conditions of both thrusters (beam voltage and thrust) on their performance figures.

Then, simplified plasma plume and target interaction models have been used to characterize numerically the momentum transfer efficiency and it has been found that, for a given mission scenario, the plume physics clearly affects the design choice. First of all, the thruster must guarantee a small initial divergence angle, as the conical beam expansion is the major factor that reduces the momentum transfer to the target and hence the efficiency of the IBS technique. Secondly, a high operational voltage also reduces the increase in divergence of the beam due to electron thermal effects.

From the point of view of the ITT alone, it is found that an optimal beam voltage (or specific impulse) exists that maximizes the transmitted force to power ratio, or equivalently that minimizes the required power for a given force on the target. Another important performance figure is however represented by the propellant mass utilization, which must guarantee a sufficiently small neutral outflow and hence a limited ion back-flow towards sensitive S/C components.

An optimization study for the overall electric propulsion subsystem has permitted to optimize the operational points of both thrusters simultaneously, finding that the minimum total dedicated mass or power are minimized for two very different operational voltages of ITT and ICT, being that of the ITT much higher. The choice on whether to minimize the total dedicated mass or the total thruster power clearly depends on the individual mission specifications.

The results presented in this paper have been used within the LEOSWEEP project to freeze the thrust and beam voltage requirements of the ITT prototype so that its design and manufacturing process could be initiated.

Acknowledgments

The research leading to the results of this paper has been carried out within the *LEOSWEEP* project and has received funding from the European Union Seventh Framework Programme (FP7/2007-2013) under grant agreement N.607457. Additional funding has been received by Spain's R&D National Plan, grant N.ESP2013-41052-P

References

[1]J.C. Liou and N.L. Johnson. A sensitivity study of the effectiveness of active debris removal in leo. *Acta Astronautica*, 64(2-3):236–243, 2009.

[2]Jasper L., Andersony P., Schaubz H., and McKnight D. Economic and risk challenges of operating in the current space debris environment. In *3rd European Workshop on Space Debris Modeling and Remediation*, CNES, Paris, 2014.

[3]C. Bombardelli and J. Peláez. Ion beam shepherd for contactless space debris removal. *Journal of Guidance, Control, and Dynamics*, 34(3):916–920, May 2011.

[4]C. Bombardelli, H. Urrutxua, M. Merino, E. Ahedo, and J. Peláez. The ion beam shepherd: A new concept for asteroid deflection. *AA*, 90(1):98 – 102, 2013.

[5]M. Merino, E. Ahedo, C. Bombardelli, H. Urrutxua, and J. Peláez. Ion beam shepherd satellite for space debris removal. In Luigi T. DeLuca, Christophe Bonnal, Oskar J. Haidn, and Sergey M. Frolov, editors, *Progress in Propulsion Physics*, volume IV of *EUCASS Advances in Aerospace Sciences*, chapter 8, pages 789–802. Torus Press, 2013.

[6]M. Ruiz, I. Urdampilleta, C. Bombardelli, E. Ahedo, M. Merino, and F. Cichocki. The FP7 LEOSWEEP project: Improving low earth orbit security with enhanced electric propulsion. In *Space Propulsion 2014*, Cologne, France, 2014.

[7]F. Cichocki, Merino M., and Ahedo E. Modeling and simulation of ep plasma plume expansion into vacuum. In *50th AIAA/ASME/SAE/ASEE Joint Propulsion Conference, Cleveland, OH*, AIAA 2014-3828, 2014.

[8]M. Merino, F. Cichocki, and E. Ahedo. Collisionless plasma thruster plume expansion model. *Plasma Sources Science and Technology*, 24(3):035006, 2015.

[9]C. Bombardelli, H. Urrutxua, M. Merino, E. Ahedo, and J. Peláez. Relative dynamics and control of an ion beam shepherd satellite. In James V. McAdams, David P. McKinley, Matthew M. Berry, and Keith L. Jenkins, editors, *Spaceflight mechanics 2012*, volume 143 of *Advances in the Astronautical Sciences*, pages 2145–2158. Univelt, 2012.

[10]D. Feili, M. Ruiz, M. Merino, F. Cichocki, E. Ahedo, M. Smirnova, and M. Dobkevicius. Impulse transfer thruster for an ion beam shepherd mission. In *34th International Electric Propulsion Conference*, IEPC-382, 2015.

[11]B.E. Beal, A. Gallimore, and J.M. Haas W.A. Hargus. Plasma properties in the plume of a hall thruster cluster. *Journal of Propulsion and Power*, 20(20):985 – 991, 2004.

[12]I.D. Boyd and J.T. Yim. Modeling of the near field plume of a Hall thruster. *Journal of applied physics*, 95:4575, 2004.

[13]J.E. Foster, G.C. Soulas, and M.J. Patterson. Plume and discharge plasma measurements of an nstar-type ion thruster. In *36th Joint Propulsion Conference and Exhibit, Huntsville, Alabama*, 2000.

[14]D.E. Parks and I. Katz. A preliminary model of ion beam neutralization. In *14th International Electric Propulsion Conference*, Fairview Park, OH, 1979. Electric Rocket Propulsion Society.